

# NONLINEAR ERROR IN EIGHT-PASS HETERODYNE INTERFEROMETERS

Chunhai Wang, Robert J. Hocken,  
Center for Precision Metrology, University of North Carolina, Charlotte

**Abstract:** Optical mixing error is one of the major concerns when using heterodyne interferometers in sub-nanometer applications. This paper focuses on optical mixing error in eight-pass interferometers. A mathematical model is built. Experimental data are obtained and compared to the model. It is found that, unlike two-pass interferometers, the eight-pass interferometer has eight error components due to optical mixing and it still takes half a wavelength displacement for the slowest component to complete a cycle of variation.

## 1. Introduction

With the advance of science and technology, the demand for sub-nanometer metrology is accelerating. Laser interferometers, a backbone in high precision metrology, are experiencing challenges. Due to the unavailability of stabilized short wavelength lasers, the resolution of interferometers is more and more dependent on the subdivision of the optical wavelength. Optical multiplexing offers an effective way to increase interferometer resolution. Eight-pass interferometers have been adopted at UNC Charlotte for a long-range scanning stage [1].

One of the major concerns when using polarization encoded heterodyne interferometers is the nonlinearity error, also called beam-mixing. Much research has been focused on the problem, mainly for two-pass interferometers [2-8]. Little work has been reported for more than two-pass interferometers. This paper will explore the optical mixing phenomenon in eight-pass interferometers. A mathematical model is developed and verified with experimental data.

## 2. Eight-pass interferometer

Figure 1 shows the configuration of an eight-pass interferometer used at UNC Charlotte. This interferometer is composed of polarizing beamsplitter PBS, two quarter-wave plates  $Q_1$  and  $Q_2$ , coated cube corner reflector CCR, measuring mirror  $M_1$ , reference mirror  $M_2$ , a roof prism and a fold mirror. A two-frequency laser (not shown in Figure 1) serves as its light source, giving two linearly polarized beams 1 and 2 with a frequency difference of about 20MHz. The CCR,  $Q_1$ ,  $Q_2$ , roof prism and fold mirror reroute the beams inside the interferometer so that beam 1 will travel four returns between PBS and  $M_1$  and beam 2 four returns between PBS to  $M_2$  before they emerge out of the interferometer. Then the two beams combine and form a heterodyne signal, which is processed by decoding electronics to calculate the displacement information.

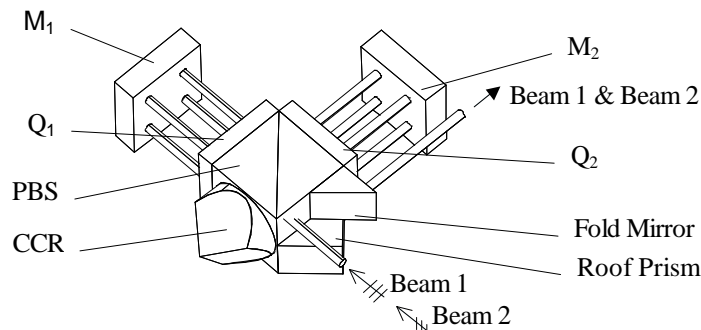


Figure 1 Eight-pass interferometer

### 3. Optical mixing error

Ideally beam 1 should travel only between PBS and  $M_1$  and beam 2 only between PBS and  $M_2$ , so that beam 1 carries the position information of  $M_1$  and beam 2 carries that of  $M_2$ . But this is based on an assumption that everything is perfect: the laser beams are perfectly linearly polarized and aligned perfectly with beamsplitter, and the beamsplitter, quarter wave plates and other optical components are perfect and aligned perfectly in the interferometer. Any imperfection will lead a beam to travel not only in the arm where it should be but also in the other arm, causing optical mixing. In this case, the optical route of a beam becomes more complex, as shown in figure 2, where  $T$  denotes a passage through PBS,  $R$  a reflection at PBS,  $Q_1$  a passage through quarter wave plate  $Q_1$ ,  $Q_2$  a passage through quarter wave plate  $Q_2$ ,  $f_1$  a round trip between  $Q_1$  and  $M_1$ ,  $f_2$  a round trip between  $Q_2$  and  $M_2$ ,  $CCR$  a reflection by CCR, and  $ROOF$  a reflection by the roof prism.

$$\begin{aligned}
 \text{Input} \rightarrow & \begin{array}{l} T \rightarrow Q_1 \rightarrow f_1 \rightarrow Q_1 \rightarrow R \\ R \rightarrow Q_2 \rightarrow f_2 \rightarrow Q_2 \rightarrow T \end{array} \xrightarrow{CCR} \begin{array}{l} R \rightarrow Q_1 \rightarrow f_1 \rightarrow Q_1 \rightarrow T \rightarrow ROOF \rightarrow T \rightarrow Q_1 \rightarrow f_1 \rightarrow Q_1 \rightarrow R \\ T \rightarrow Q_2 \rightarrow f_2 \rightarrow Q_2 \rightarrow R \rightarrow ROOF \rightarrow R \rightarrow Q_2 \rightarrow f_2 \rightarrow Q_2 \rightarrow T \end{array} \rightarrow \\
 & \begin{array}{l} \rightarrow CCR \rightarrow R \rightarrow Q_1 \rightarrow f_1 \rightarrow Q_1 \rightarrow T \\ T \rightarrow Q_2 \rightarrow f_2 \rightarrow Q_2 \rightarrow R \end{array} \rightarrow \text{Output}
 \end{aligned}$$

Figure 2 Optical route of a laser beam in the eight-pass interferometer

To calculate the optical mixing, the Jones Matrices are employed. Following the optical route in figure 2, the eight-pass interferometer can be described as:

$$\begin{aligned}
 \mathbf{J} = & (\mathbf{J}_{thru} \underbrace{\mathbf{J}_{1/4} \mathbf{J}_{f_1} \mathbf{J}_{1/4}}_{4\text{th travel to M1}} \mathbf{J}_{refl} + \mathbf{J}_{refl} \underbrace{\mathbf{J}_{1/4} \mathbf{J}_{f_2} \mathbf{J}_{1/4}}_{4\text{th travel to M2}} \mathbf{J}_{thru}) \mathbf{J}_{ccr} (\mathbf{J}_{refl} \underbrace{\mathbf{J}_{1/4} \mathbf{J}_{f_1} \mathbf{J}_{1/4}}_{3\text{rd travel to M1}} \mathbf{J}_{thru} \mathbf{J}_{roof} \mathbf{J}_{thru} \underbrace{\mathbf{J}_{1/4} \mathbf{J}_{f_1} \mathbf{J}_{1/4}}_{2\text{nd travel to M1}} \mathbf{J}_{refl} \\
 & + \mathbf{J}_{thru} \underbrace{\mathbf{J}_{1/4} \mathbf{J}_{f_2} \mathbf{J}_{1/4}}_{3\text{rd travel to M2}} \mathbf{J}_{refl} \mathbf{J}_{roof} \mathbf{J}_{refl} \underbrace{\mathbf{J}_{1/4} \mathbf{J}_{f_2} \mathbf{J}_{1/4}}_{2\text{nd travel to M2}} \mathbf{J}_{thru}) \mathbf{J}_{ccr} (\mathbf{J}_{refl} \underbrace{\mathbf{J}_{1/4} \mathbf{J}_{f_1} \mathbf{J}_{1/4}}_{1\text{st travel to M1}} \mathbf{J}_{thru} + \mathbf{J}_{thru} \underbrace{\mathbf{J}_{1/4} \mathbf{J}_{f_2} \mathbf{J}_{1/4}}_{1\text{st travel to M2}} \mathbf{J}_{refl}) \quad (1)
 \end{aligned}$$

where  $\mathbf{J}_{thru}$  denotes the Jones matrix for a passage through PBS,  $\mathbf{J}_{refl}$  the Jones Matrix for a reflection by PBS,  $\mathbf{J}_{1/4}$  the Jones matrix for quarter wave plate  $Q_1$  and  $Q_2$ ,  $\mathbf{J}_{f_1}$  the Jones matrix for a round travel between  $M_1$  and  $Q_1$ ,  $\mathbf{J}_{f_2}$  the Jones matrix for a round travel between  $Q_2$  and  $M_2$ ,  $\mathbf{J}_{ccr}$  the Jones matrix for coated cube corner reflector CCR, and  $\mathbf{J}_{roof}$  the Jones Matrix for the roof prism. Since the two laser beams are only 20MHz different in frequency, they see virtually the same polarizing effect when propagating in the interferometer. Some Jones Matrix value for both the ideal and non-ideal optical components are shown in Table 1.

Table 1 Jones Matrices

Symbol	$\mathbf{J}_{thru}$	$\mathbf{J}_{refl}$	$\mathbf{J}_{1/4}$	$\mathbf{J}_{f_1}$	$\mathbf{J}_{f_2}$	$\mathbf{J}_{ccr}$	$\mathbf{J}_{roof}$
Ideal components	$\begin{bmatrix} 1 & 0 \\ 0 & 0 \end{bmatrix}$	$\begin{bmatrix} 0 & 0 \\ 0 & 1 \end{bmatrix}$	$\begin{bmatrix} 0.5 + 0.5i & 0.5 - 0.5i \\ 0.5 - 0.5i & 0.5 + 0.5i \end{bmatrix}$	$\begin{bmatrix} e^{if_1} & 0 \\ 0 & e^{if_1} \end{bmatrix}$	$\begin{bmatrix} e^{if_2} & 0 \\ 0 & e^{if_2} \end{bmatrix}$	$\begin{bmatrix} 1 & 0 \\ 0 & 1 \end{bmatrix}$	$\begin{bmatrix} 1 & 0 \\ 0 & 1 \end{bmatrix}$
Non-ideal components	$\begin{bmatrix} 1 & 0 \\ 0 & \mathbf{a} \end{bmatrix}$	$\begin{bmatrix} \mathbf{a} & 0 \\ 0 & 1 \end{bmatrix}$					

Let  $\mathbf{E}_1$  and  $\mathbf{E}_2$  denote the Jones vectors for input beam 1 and 2, the polarizing effect of the interferometer on the two beams can be expressed as

$$\mathbf{E}'_1 = \mathbf{J}\mathbf{E}_1 \quad (2)$$

$$\mathbf{E}'_2 = \mathbf{J}\mathbf{E}_2 \quad (3)$$

The heterodyne signal is formed by synthesizing  $E_1$  and  $E_2$ . Restoring the time dependence, the electric field of the heterodyne signal will possess the mathematical form

$$E_h = E_{14}e^{-i(\omega_1 t + 4f_1)} + \mathbf{e}_{13}e^{-i(\omega_1 t + 3f_1 + f_2)} + \mathbf{e}_{12}e^{-i(\omega_1 t + 2f_1 + 2f_2)} + \mathbf{e}_{11}e^{-i(\omega_1 t + f_1 + 3f_2)} + \mathbf{e}_{10}e^{-i(\omega_1 t + 4f_2)} \\ + E_{24}e^{-i(\omega_2 t + 4f_2)} + \mathbf{e}_{23}e^{-i(\omega_2 t + 3f_2 + f_1)} + \mathbf{e}_{22}e^{-i(\omega_2 t + 2f_2 + 2f_1)} + \mathbf{e}_{21}e^{-i(\omega_2 t + f_2 + 3f_1)} + \mathbf{e}_{20}e^{-i(\omega_2 t + 4f_1)} \quad (4)$$

where  $\omega_1$  is the angular frequency of beam 1,  $\omega_2$  is the angular frequency of beam 2,  $E_{14}$  denotes the amplitude of the light component that originates from beam 1 and travels 4 returns only between PBS and  $M_1$ ,  $\mathbf{e}_k$  ( $k = 1, 2, 3, 4$ ) the light components that originate from beam 1 and travel  $4-k$  returns between PBS and  $M_1$  and  $k$  returns between PBS and  $M_2$ ,  $E_{24}$  is the amplitudes of the light components that originates from beam 2 and travels 4 returns only between PBS and  $M_2$ , and  $\mathbf{e}_{2k}$  ( $k = 1, 2, 3, 4$ ) the amplitudes of the light components that originate from beam 2 and travel  $4-k$  returns between PBS and  $M_2$  and  $k$  returns between PBS and  $M_1$ . The intensity of the heterodyne signal is

$$I \propto |E_h|^2 = |E_{14}|^2 + |\mathbf{e}_{13}|^2 + |\mathbf{e}_{12}|^2 + |\mathbf{e}_{11}|^2 + |\mathbf{e}_{10}|^2 + |E_{24}|^2 + |\mathbf{e}_{23}|^2 + |\mathbf{e}_{22}|^2 + |\mathbf{e}_{21}|^2 + |\mathbf{e}_{20}|^2 \\ + 2E_{14}E_{24} \cos[(\omega_1 - \omega_2)t + 4(\mathbf{f}_1 - \mathbf{f}_2)] \\ + 2(E_{14}\mathbf{e}_{23} + E_{24}\mathbf{e}_{13}) \cos[(\omega_1 - \omega_2)t + 3(\mathbf{f}_1 - \mathbf{f}_2)] \\ + 2(E_{14}\mathbf{e}_{22} + E_{24}\mathbf{e}_{12} + \mathbf{e}_{13}\mathbf{e}_{23}) \cos[(\omega_1 - \omega_2)t + 2(\mathbf{f}_1 - \mathbf{f}_2)] \\ + 2(E_{14}\mathbf{e}_{21} + E_{24}\mathbf{e}_{11} + \mathbf{e}_{12}\mathbf{e}_{23} + \mathbf{e}_{13}\mathbf{e}_{22}) \cos[(\omega_1 - \omega_2)t + (\mathbf{f}_1 - \mathbf{f}_2)] \\ + 2(E_{14}\mathbf{e}_{20} + E_{24}\mathbf{e}_{10} + \mathbf{e}_{11}\mathbf{e}_{23} + \mathbf{e}_{12}\mathbf{e}_{22} + \mathbf{e}_{13}\mathbf{e}_{21}) \cos[(\omega_1 - \omega_2)t] \\ + 2(\mathbf{e}_{12}\mathbf{e}_{21} + \mathbf{e}_{13}\mathbf{e}_{20} + \mathbf{e}_{11}\mathbf{e}_{22} + \mathbf{e}_{10}\mathbf{e}_{23}) \cos[(\omega_1 - \omega_2)t - (\mathbf{f}_1 - \mathbf{f}_2)] \\ + 2(\mathbf{e}_{11}\mathbf{e}_{21} + \mathbf{e}_{12}\mathbf{e}_{20} + \mathbf{e}_{10}\mathbf{e}_{22}) \cos[(\omega_1 - \omega_2)t - 2(\mathbf{f}_1 - \mathbf{f}_2)] \\ + 2(\mathbf{e}_{11}\mathbf{e}_{20} + \mathbf{e}_{10}\mathbf{e}_{21}) \cos[(\omega_1 - \omega_2)t - 3(\mathbf{f}_1 - \mathbf{f}_2)] \\ + 2\mathbf{e}_{10}\mathbf{e}_{20} \cos[(\omega_1 - \omega_2)t - 4(\mathbf{f}_1 - \mathbf{f}_2)] \\ + 2E_{14} \sum_{k=0}^3 \mathbf{e}_{1k} \cos[(4-k)(\mathbf{f}_1 - \mathbf{f}_2)] + 2E_{24} \sum_{k=0}^3 \mathbf{e}_{2k} \cos[(4-k)(\mathbf{f}_1 - \mathbf{f}_2)] \\ + 2 \sum_{j=0}^3 \sum_{k=0}^j \mathbf{e}_{1j}\mathbf{e}_{1k} \cos[(j-k)(\mathbf{f}_1 - \mathbf{f}_2)] + 2 \sum_{j=0}^3 \sum_{k=0}^j \mathbf{e}_{2j}\mathbf{e}_{2k} \cos[(j-k)(\mathbf{f}_1 - \mathbf{f}_2)] \quad (5)$$

The right hand side of the first line is the DC component, the second line is the main heterodyne signal, the third to the tenth are optical mixing signals, and the last two lines are quasi-DC components. Usually the DC and quasi-DC components are filtered away by the electronics, and the high frequency signals (line 2 to line 10) are left. Nonlinear error can be expressed in angular phase, which is equal to the sum of optical mixing components (line 3 to 10) divided by the main heterodyne signal. In the worst case, it is the sum of the amplitudes from line 3 to 10 divided by the amplitude in line 2. The smaller  $\mathbf{e}_{13}, \mathbf{e}_{12}, \mathbf{e}_{11}, \mathbf{e}_{10}, \mathbf{e}_{23}, \mathbf{e}_{22}, \mathbf{e}_{21}$  and  $\mathbf{e}_{20}$ , the smaller the nonlinear error. We can also note that different mixing components have different periodicities. The line 10 signal takes  $1/8$  wavelength displacement ( $4(\mathbf{f}_1 - \mathbf{f}_2) = 2\pi$ ) to complete a cycle while line 3 and 9 take  $1/6$  wavelength displacement ( $3(\mathbf{f}_1 - \mathbf{f}_2) = 2\pi$ ), line 4 and 6 take  $1/4$  wavelength displacement ( $2(\mathbf{f}_1 - \mathbf{f}_2) = 2\pi$ ), and line 5 and line 7, the slowest error components, take  $1/2$  wavelength displacement ( $(\mathbf{f}_1 - \mathbf{f}_2) = 2\pi$ ), that is to say, a complete nonlinear error cycle in eight-pass interferometer will be  $1/2$  wavelength displacement.

To verify equation (5), an experiment was designed. According to equation (5), if measuring mirror  $M_1$  is moved at a constant speed, equation (5) will present nine spectral lines (line 2 to 10). Adjacent frequencies are spaced by  $v/\lambda$ , where  $\lambda$  is the mean wavelength of the two frequency laser and  $v$  the velocity of  $M_1$ . The measured spectrum is shown in figure 3. The largest peak 1 in the figure is the main heterodyne signal, corresponding to the term in line 2 of equation (5). Other significant peaks 2,

3, 4 and 5 correspond to the error terms in line 3, 4, 6 and 10 respectively. The error terms in line 5, 7, 8 and 9 are not significant in this interferometer. Nonlinear error, by figure 3, is about 0.039 radians in phase corresponding to a displacement error about 0.5nm.

Various imperfections that might affect optical mixing errors were analyzed based on the model. Details will not be given here due to length constraints. It was found that the optical mixing errors are more sensitive to the misalignment between the laser polarization orientation and the beamsplitter, but less sensitive to the imperfections of the beamsplitter. Slight misalignment and imperfection of quarter wave plates theoretically have no contribution to optical mixing errors.

#### 4. Summery

A mathematical model was developed to study optical mixing errors in an eight-pass interferometer. An experimental spectrum was compared to the model. It was found that the eight-pass interferometer has eight optical mixing components and a complete cycle of the slowest mixing component requires a measurement mirror displacement of 0.5 Wavelengths. The influence of misalignment and imperfection of the optical components on the nonlinear error is slightly different from that of a two-pass interferometer.

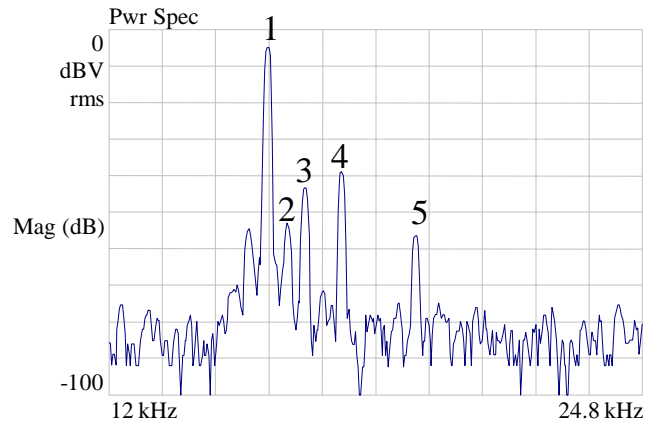


Figure 3 The spectrums of heterodyne signal

#### 5. Acknowledgments

The research is funded by the National Science Foundation under the grant No.2975990126, and carried out in the Center for Precision Metrology, University of North Carolina at Charlotte.

#### 6. Reference

- [1] Mike Holmes, Robert Hocken, David Trumper, "The long-range scanning stage: a novel platform for scanned-probe microscopy", *Precision Engineering*, Vol. 24, No. 3, 2000, pp 191-209
- [2] Bobroff N, "Recent advances in displacement measuring interferometry", *Measurement Science and Technology*, Vol 4, No. 9, 1993 pp.907-926
- [3] Tanaka M., Yamagami T., and Nakayama K., "Linear interpolation of periodic error in a heterodyne laser interferometer at subnanometer level", *IEEE Trans. Instrum. Meas.*, Vol. 38, No.2, 1989, pp552-554
- [4] Hou W., and Wilkening G., "Investigation and compensation of the nonlinearity of heterodyne interferometers", *Precision Engineering*, Vol. 16, No. 1, 1994, pp25-35
- [5] Badami, V. G., "Investigation and compensation of periodic nonlinearities in heterodyne interferometry", PhD's Thesis, Department of Mechanical Engineering and Engineering Science, UNCC Charlotte, NC, 1999
- [6] Bobroff N., "Residual errors in laser interferometry from air turbulence and nonlinearity", *Appl. Opt.*, Vol. 26, No. 13, 1987, pp2676-2682
- [7] J.A. Stone, L.P. Howard, A simple technique for observing periodic nonlinearities in Michelson interferometers, *Precision Engineering* Vol. 22, No. 4, 1998, pp. 220-232.
- [8] V.G. Badami, S.R. Patterson, A frequency domain method for the measurement of nonlinearity in heterodyne interferometry, *Precision Engineering* Vol. 24, No. 1, 2000, pp. 41-49.